Surface Scatter Phenomena: A Linear, Shift-Invariant Process

James Harvey

James E. Harvey, "Surface Scatter Phenomena: A Linear, Shift-Invariant Process," Proc. SPIE 1165, Scatter from Optical Components, (2 January 1990); doi: 10.1117/12.962839

SPIE.

Event: 33rd Annual Technical Symposium, 1989, San Diego, United States

Surface scatter phenomena: a linear, shift-invariant process

James E. Harvey

The Perkin-Elmer Corporation
100 Wooster Hts. Rd., M/S 813
Danbury, Connecticut 06810

ABSTRACT

Empirical experimental scattering data from conventional optical surfaces is shown to exhibit shift-invariant behavior with respect to incident angle when plotted in direction cosine space. This implies the existence of a surface transfer function that completely characterizes the scattering properties of the surface, and permits the application of linear systems theory and Fourier techniques in modeling the scattering effects of optical surfaces. A theoretical basis for this behavior is illustrated by showing that scalar diffraction phenomena (conical diffraction from gratings) is shift-invariant with respect to incident angle only in direction cosine space, and surface roughness can be considered to be composed of a superposition of sinusoidal phase gratings. The fact that many optical surfaces of interest deviate from this shift-invariant behavior does not invalidate the usefulness of the linear systems formalism. The ideal behavior of a shift-invariant scattering process can still be used for making engineering calculations and retained as the reference from which scattering from real surfaces is compared. This is completely analogous to the universally accepted transfer function characterization of imaging systems in spite of the fact that few real imaging systems are isoplanatic (no field-dependent aberrations).

1. INTRODUCTION

The effects of light scattered from optical surfaces has received considerable attention in recent years, as evidenced in the increasing number of conferences devoted to the subject.[1-8] In many applications it is not only the amount of scattered light, but also the direction of the scattered radiation that plays a crucial role in the performance of the system. This is particularly true in the design and analysis of stray light rejection systems required by optical instruments used to view a relatively faint target in the vicinity of a much brighter object.

It is well known that the angular distribution of scattered light, or bidirectional reflectance, from an optical surface changes with variations in the angle of incidence. Nicodemus has discussed this problem in detail and defined the bidirectional reflectance distribution function (BRDF) that completely describes the scattering properties of a surface.[9] The BRDF is a four-dimensional (azimuth and elevation angles for both the incident and reflected directions) quantity that can be thought of as an infinite family of two-dimensional scattered light distribution functions--one for every possible angle at which the incident beam can strike the surface. To experimentally characterize the complete BRDF of an optical surface would, in general, involve an overwhelming quantity of data, especially if high directional resolution is needed to describe glints and specularities.

This paper is intended to be a tutorial on the application of linear systems theory to surface scatter phenomena and was motivated in part by paper 1165-02 in this conference proceedings.[10] The resulting model is analogous to, and an extension of, the highly successful application of linear systems theory to the understanding of image forming systems. A theoretical basis for presenting scattering (BRDF) data in direction cosine space is presented by showing that wide-angle diffraction phenomena are shift-invariant with respect to incident angle only when formulated in terms of the direction cosines of the propagation vectors. Some angular scattering data is then presented in a format which indicates that the scattering process from a certain class of optical surfaces is indeed shift-invariant with respect to incident angle. This leads to the derivation of a "surface transfer function" which relates the scattering properties to the surface topography and a simple wavelength scaling law (which is validated experimentally). The fact that not all scattering surfaces of interest exhibit this convenient behavior does **not** invalidate the usefulness of the model. This simple scalar model still provides for useful engineering calculations of scattered radiation and an idealized behavior from which to measure the departure of actual performance (similar to describing the field-dependent aberrations of

nonisoplanatic imaging systems). Only by plotting measured BRDF data in the format suggested here does it becomes obvious which real surfaces exhibit the shift-invariant behavior necessary to allow using this simple model with confidence. If departures from shift-invariant behavior are severe or if polarization effects are significant for the application at hand, then a more rigorous (vector) theoretical treatment is obviously required.[11-13] However, I emphasize my conviction that it is always good engineering practice to use the simplest theory available that adequately describes the phenomenon of concern.

2. LINEAR SYSTEMS THEORY

In the analysis of any physical system or process, it is necessary to develop a model that describes the behavior of the system mathematically. Models for describing real physical phenomena will almost always be an idealization, but they can still be a very useful analysis and simulation tool as long as their limitations are understood and taken into account.

A systems approach to modeling physical phenomena often makes use of mathematical operators which produce the system output when applied to the system input as illustrated in Figure 1a. The condition for linearity is given by

$$L[a_1 f_1(x, y) + a_2 f_2(x, y)] = a_1 L[f_1(x, y)] + a_2 L[f_2(x, y)] \quad (1)$$

If, in addition, the system is shift-invariant (i.e., when the input is shifted, the output is merely shifted without a change in functional form)

$$L[f(x - xo, y - yo)] = g(x - xo, y - yo) \quad (2)$$

then we have the linear, shift-invariant (LSI) system illustrated schematically in Figure 1b. The output of an LSI system is given by convolving the input with the system impulse response, or upon applying the convolution theorem of Fourier transform theory, the output spectrum of the system is given by the product of the input spectrum with the system transfer function.[14]

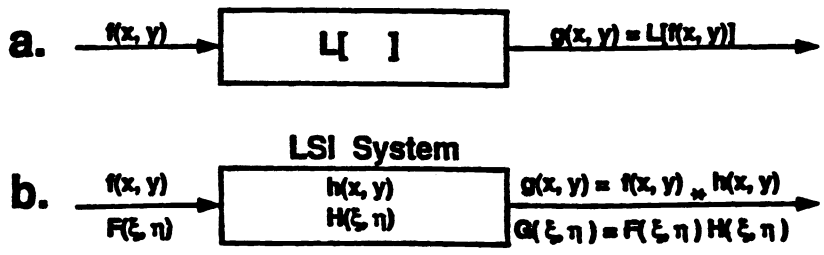

Figure 1 a. General system characterized by a mathematical operator
b. LSI system characterized by a system transfer function

LSI systems can thus be completely characterized by the system transfer function which is defined as the ratio of the output spectrum to the input spectrum

$$\text{Transfer Function} = H(\xi, \eta) = G(\xi, \eta)/F(\xi, \eta) \quad (3)$$

3. MODERN IMAGE FORMATION THEORY

Linear systems theory and the associated system transfer function have been widely applied to the characterization of imaging systems.[14-18] Figure 2 schematically illustrates an imaging system represented as a "black box" with a two-dimensional input "object" distribution and a two-dimensional output "image" distribution.

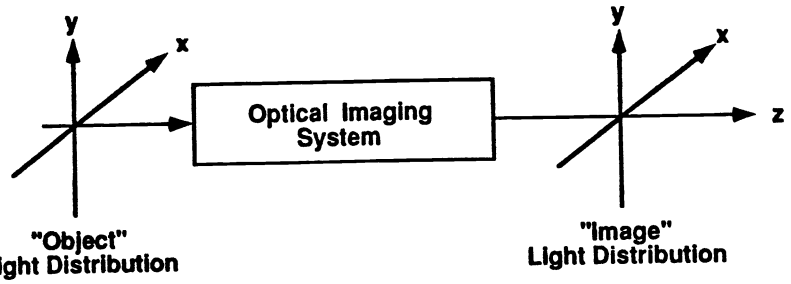

Figure 2. Systems approach to modeling a general imaging system.

If field-dependent aberrations are ignored, an imaging system can be treated as an LSI system and characterized by an optical transfer function (OTF). The optical transfer function is given by the normalized autocorrelation of the complex pupil function, the point spread function is given by the squared modulus of the Fourier transform of the complex pupil function, and from the autocorrelation theorem from Fourier transform theory, the OTF and the PSF are Fourier transforms of each other. These relationships are shown in Figure 3 along with a variety of commonly used image quality criteria.

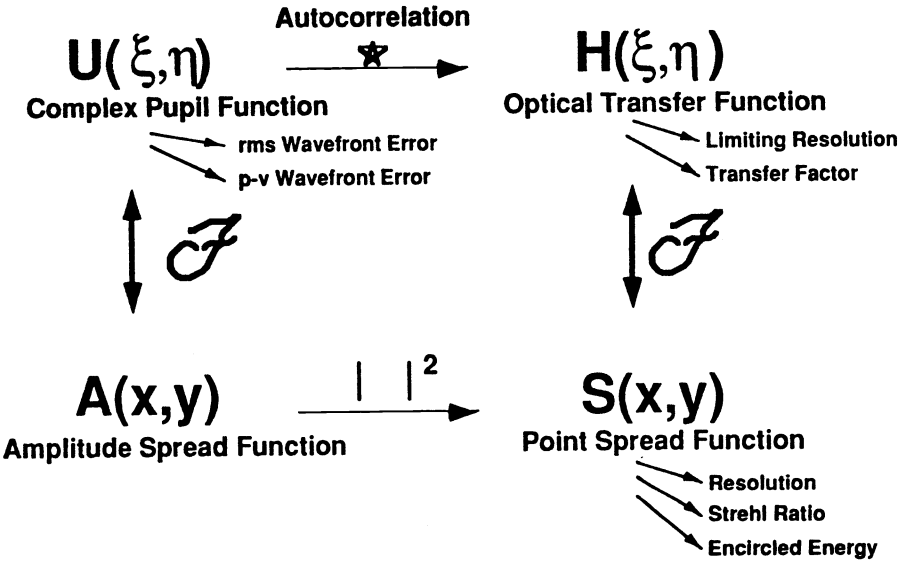

Figure 3. Relationship between the complex pupil function, optical transfer function, and the point spread function.

The optical transfer function or its modulus, the modulation transfer function (MTF), has gained almost universal acceptance as the image quality criterion of choice for a wide range of imaging applications involving diffraction-limited optics or those suffering from aberrations (in spite of the fact that field-dependent aberrations destroy the shift invariance). Further image degradation due to image motion has also been modeled by an appropriate transfer function for image jitter and drift.[19,20]

4. SCALAR DIFFRACTION THEORY

It is well known that the complex amplitude distribution in the far field (Fraunhofer region) of a diffracting aperture is given by the Fourier transform of the complex amplitude transmittance of the diffracting aperture, and that the Fresnel diffraction integral is just the Fourier transform of the product of the aperture function with a quadratic phase factor.[18] However, Harvey has shown that the rigorous Rayleigh-Sommerfeld diffraction integral (valid in the near field) can be written as the Fourier transform of a generalized pupil function that contains phase variations which resemble conventional aberrations.[21] When a spherical wave is incident upon a diffracting aperture and the observation space

is a hemisphere centered upon the diffracting aperture as shown in Figure 4, these phase variations are frequently negligible and the diffracted wave field on the hemisphere is then given directly by the Fourier transform of the pupil function

$$U(\alpha, \beta; \hat{r}) = \gamma\,[\exp(i2\pi\,\hat{r})/(i\hat{r})]\;\mathcal{F}\{U_o(\hat{x}, \hat{y}; 0)\} \tag{4}$$

And furthermore, this Fourier transform relationship is valid not merely over a small region about the optical axis, but over the *entire hemisphere* (with certain restrictions depending upon the residual phase variations). Note that a scaled coordinate system has been utilized in which all of the spatial variables are normalized by the wavelength of the light

$$\hat{x} = x/\lambda, \hat{y} = y/\lambda, \hat{z} = z/\lambda, \text{ etc.} \tag{5}$$

and the direction cosines α and β of the position vector of the observation point are the reciprocal variables in the Fourier transform space

$$\alpha = \hat{x}/\hat{r}, \beta = \hat{y}/\hat{r}, \text{ and } \gamma = \hat{z}/\hat{r} \tag{6}$$

As we will see, this *direction cosine space* is a very convenient space in which to discuss the diffraction process.

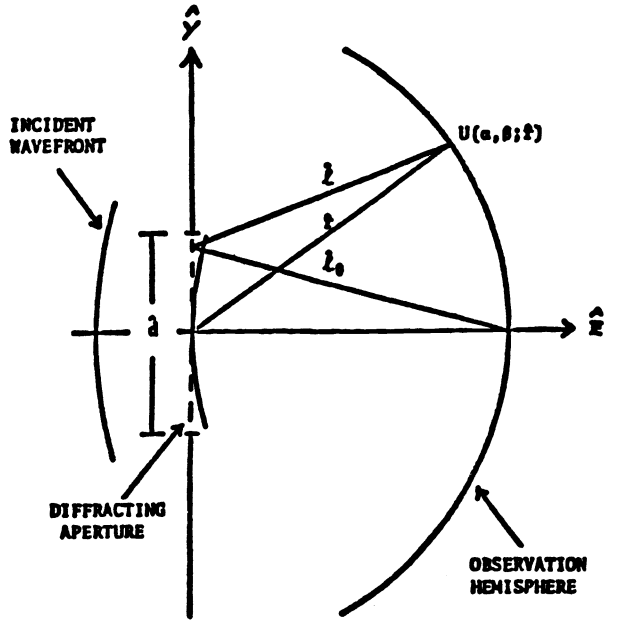

Figure 4. Geometrical relationship between incident beam, diffracting aperture, and observation hemisphere.

Now consider the situation where where the incident radiation strikes the diffracting aperture at an angle θ_o as illustrated in Figure 5. This is equivalent to introducing a linear phase variation across the aperture. By applying the shift theorem of Fourier transform theory to Eq. (4) we find that the complex amplitude distribution on the hemisphere is a function of $\beta - \beta_o$,

$$U(\alpha, \beta - \beta_o; \hat{r}) = \gamma\,[\exp(i2\pi\,\hat{r})/(i\hat{r})]\;\mathcal{F}\{U_o(\hat{x}, \hat{y}; 0)\,\exp(i2\pi\beta_o\,\hat{y})\} \tag{7}$$

where β is the direction cosine of the position vector of the observation point, and β_o is the direction cosine of the position vector of the undiffracted beam.[22] Note that the direction cosines are obtained by merely projecting the respective points on the hemisphere back onto the plane of the aperture and normalizing to a unit radius. The complex amplitude distribution at an arbitrary point on the hemisphere can now be said to be a function of the *distance of the observation point from the undiffracted beam in direction cosine space.*

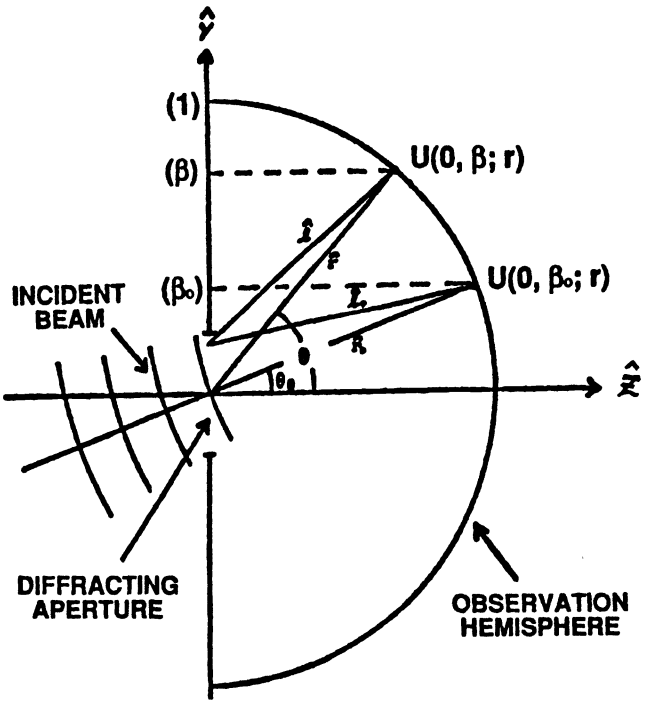

Figure 5. Geometrical configuration when the incident beam strikes the diffracting aperture at an arbitrary angle.

As a specific example, consider diffraction from a conventional linear grating. Suppose we have incident light striking a diffraction grating at an oblique angle (represented by direction cosines α_i and β_i) as illustrated in Figure 6. The grating equation for an arbitrary (skew) obliquely incident beam is very simply written in direction cosine space (the grooves are assumed to be parallel to the y axis)

$$\alpha_m + \alpha_i = m\lambda/d$$
$$\beta_m + \beta_i = 0 \qquad (8)$$

where

$$\alpha_m = \sin\theta_m \cos\phi_o$$
$$\alpha_i = -\sin\theta_o \cos\phi_o \qquad (9)$$
$$\beta_i = -\sin\phi_o$$

The diffracted orders will propagate along the surface of a cone (thus sometimes referred to as conical diffraction) and will strike the observation hemisphere in a cross section which is not a great circle but instead a latitude slice. For large angles of incidence and large diffracted angles the various orders appear to be equally spaced and lie on a straight line only if they are projected down onto the α–β plane in direction cosine space. This behavior is even more evident in Figure 7 in which the location of the incident beam and the diffracted orders are displayed in direction cosine space for a grating whose grooves are parallel to the y axis. Note that the diffracted orders are always equally spaced and lie in a straight line parallel to the α axis in direction cosine space. Those diffracted orders that lie inside the unit circle are real and propagate whereas the diffracted orders that lie outside the unit circle are evanescent. The zero or undiffracted order always lies diametrically opposite the origin of the $\alpha - \beta$ coordinate system from the incident beam. As the incident angle is varied, the diffraction pattern (size, shape, separation, and orientation of diffracted orders) remains unchanged but merely shifts its position maintaining the above relationship between the undiffracted order and the incident beam.

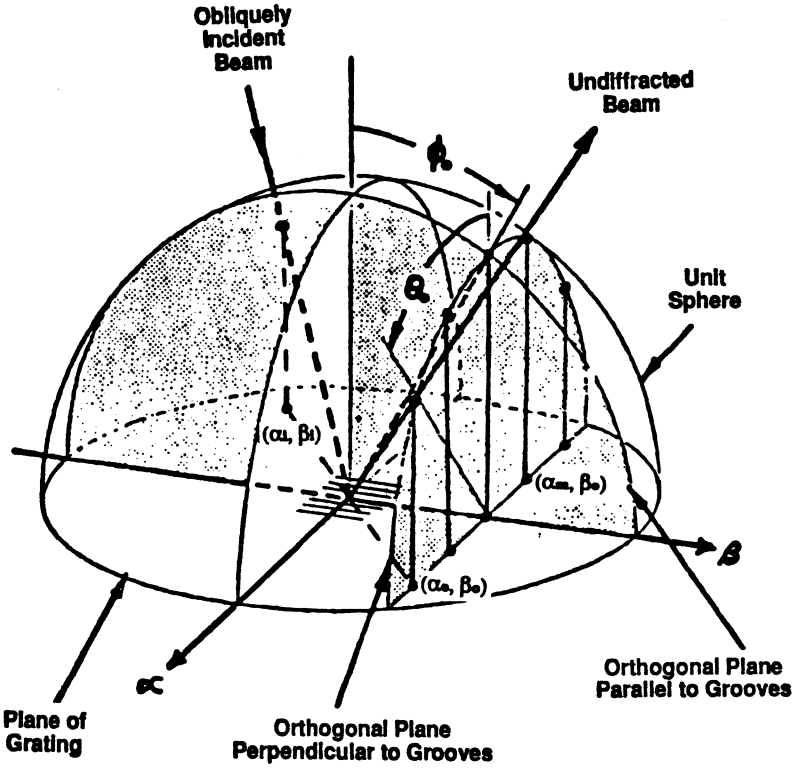

Figure 6. Illustration of the position of the diffracted orders in real space and direction cosine space for an arbitrary (skew) obliquely incident beam.

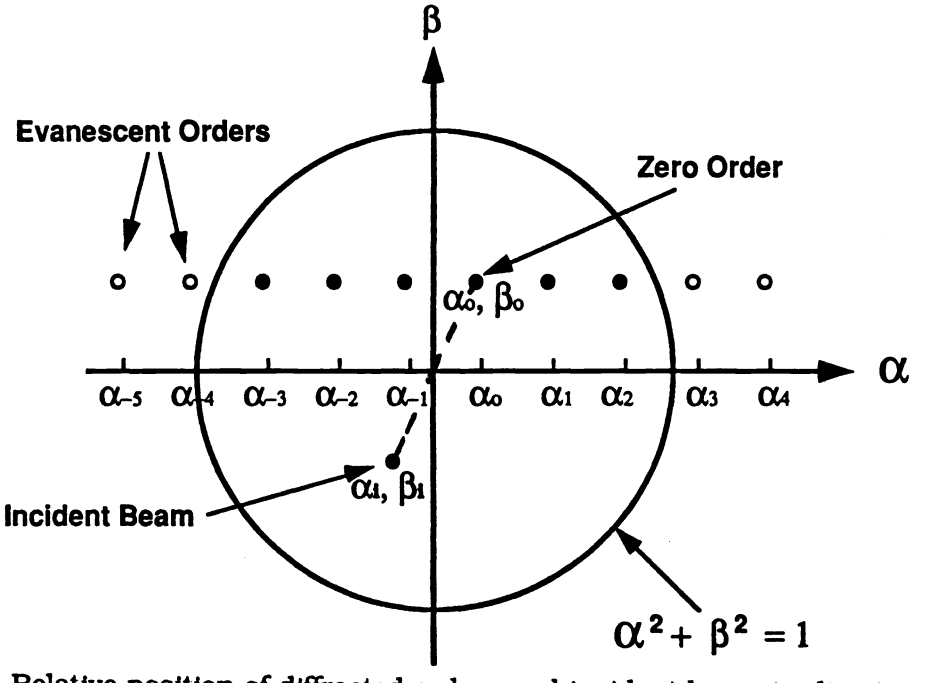

Figure 7. Relative position of diffracted orders and incident beam in direction cosine space. Diffracted orders outside the unit circle are evanescent.

When the plane of incidence is parallel to the grating grooves ($\phi_o = 0$), Eq.(8) reduces to the more familiar form of the grating equation

$$\sin \theta_m + \sin \theta_i = m\lambda/d \qquad (10)$$

A final demonstration that diffraction phenomena are most simply expressed in direction cosine space follows. In Figure 8a the diffraction angle is plotted versus incident angle for a diffraction grating with $\lambda/d = 0.76$. Note that the angular separation of the diffracted orders varies drastically with incident angle. In Figure 8b the behavior of the same grating is illustrated in direction cosine space. Here the separation of the diffracted orders is invariant with incident angle and the entire diffraction pattern merely shifts in direction space, without changing its functional form as the incident angle is changed.

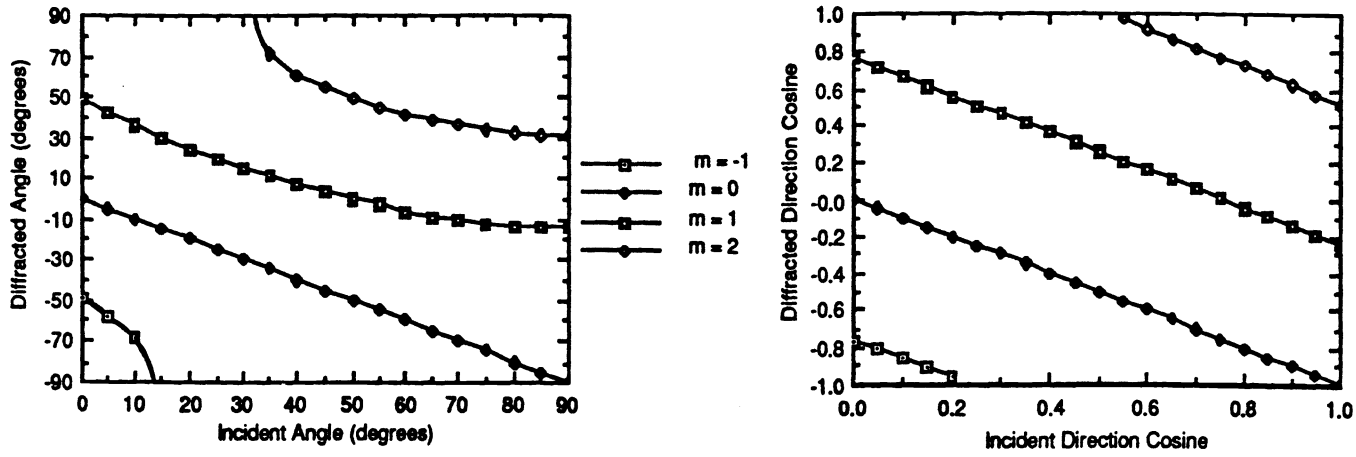

Figure 8. Diffraction patterns from simple linear gratings are shift-invariant only in direction cosine space.

5. SURFACE SCATTER PHENOMENA

It is customary to present angular scattering data as scattered intensity (flux per unit solid angle) versus scattering angle. Figure 9 illustrates several scattered light profiles from a polished and aluminized fused quartz sample. The results confirm the well-known fact that the scattered light distribution changes shape drastically with angle of incidence, becoming quite skewed and asymmetrical at large angles of incidence.

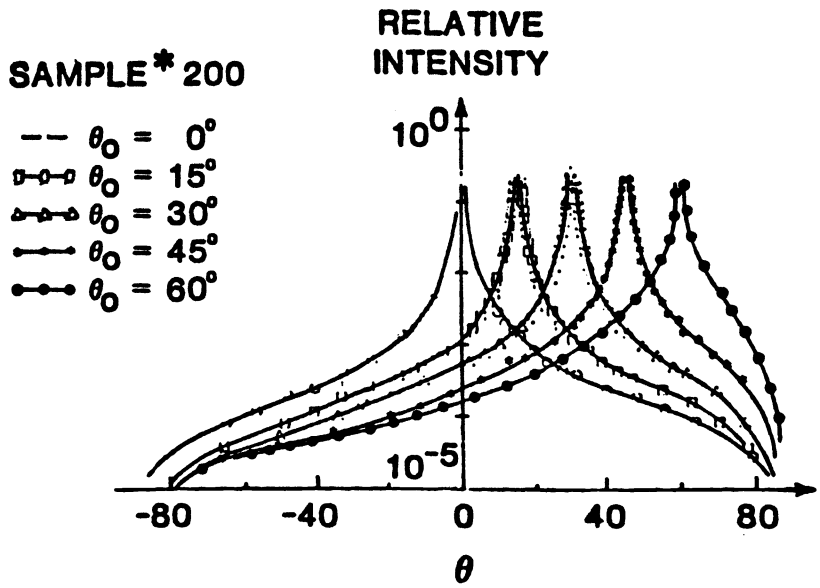

Figure 9. Scattered intensity versus scattering angle.

The bidirectional reflectance distribution function (BRDF), defined as the reflected radiance (radiant power per unit solid angle per unit projected area) in a given direction divided by the incident irradiance (radiant power per unit area) is widely used to describe such scattering behavior.[9]

$$BRDF\,|_{\theta i,\phi i} = f(\theta_r, \phi_r; \theta_i, \phi_i) = dL_r(\theta_r, \phi_r; \theta_i, \phi_i) / dE_i(\theta_i, \phi_i) \qquad (11)$$

This fundamental quantity is a function of the angles of reflectance, (θ_r,ϕ_r), and the angles of incidence, (θ_i,ϕ_i), as well as the wavelength of the incident radiation and the state of polarization of both the incident and reflected waves. The angles used in the above definition are illustrated in Figure 10.

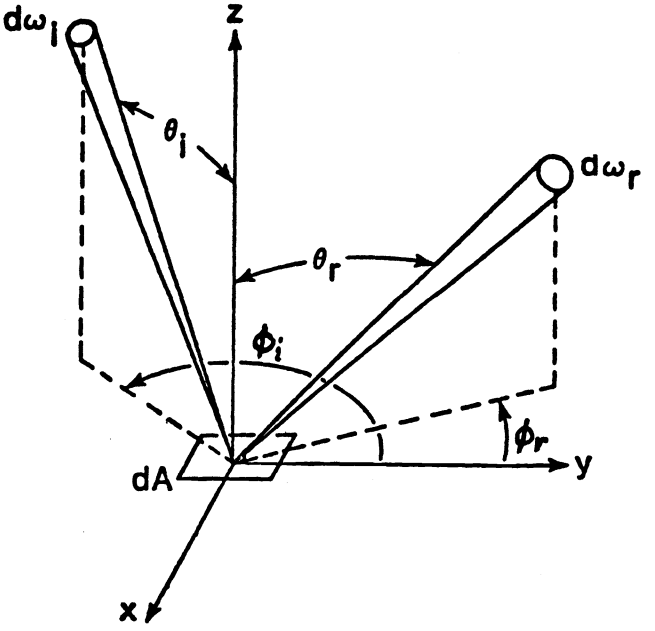

Figure 10. Illustration of scattering geometry

For a narrow beam at a fixed angle of incidence, we can drop the differentials and approximate the resulting quantity as

$$BRDF\,|_{\theta i,\phi i} = L_r(\theta_r, \phi_r; \theta_i, \phi_i) / E_i(\theta_i,\phi_i) = [dP(\theta_r, \phi_r)/d\omega\ \Delta A \cos\theta]/[P_o/\Delta A] \qquad (12)$$

where $P_o = P/R$ is the total power incident upon the illuminated area ΔA of the scattering surface and R is the Fresnel reflectance of the surface (and hence contains a wavelength, incident angle, and a polarization dependance). Recalling that $I(\alpha, \beta) = dP/d\omega$ and $\gamma = \cos\theta$, we obtain

$$BRDF\,|_{\theta i,\phi i} = [R/\gamma P]\, I(\alpha, \beta) = R\mathcal{S}(\alpha, \beta) \qquad (13)$$

where this scattered radiance distribution function $\mathcal{S}(\alpha, \beta)$ depends implicitly upon the angle of incidence.[23] Thus the total four-dimensional BRDF can accurately be thought of as an infinite family of two-dimensional scattering functions, one for every possible angle of the incident beam.

If we now take the relative scattered intensity, $I(\alpha, \beta)/P_o$, measured in the plane of incidence ($\phi_i = \pi$, $\phi_r = \phi_o = 0$), illustrated in Figure 9 and divide by the cosine of the scattering angle, $\gamma = \cos\theta$, then replot as a function of $\beta-\beta_o$, where $\beta = \sin\theta$ and $\beta_o = \sin\theta_o$, the five curves with the incident angles varying form zero to 60 degrees coincide almost perfectly as shown in Figure 11. This shift-invariant behavior drastically reduces the quantity of data required to completely characterize the scattering properties of the surface.

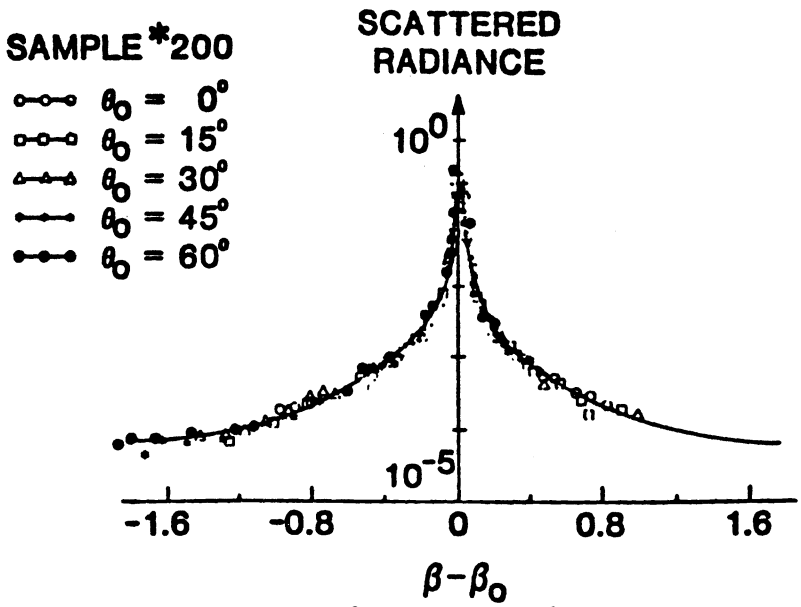

Figure 11. Scattered radiance is shift-invariant in direction cosine space.

Scattered light data is usually collected on an observation hemisphere with some type of goniometric instrument. Figure 12 shows an incident beam striking a scattering surface at some angle of incidence ($\theta_i = -\theta_o$), a specularly reflected beam striking the observation hemisphere at the position indicated, and the scattered intensity distribution being sampled at an arbitrary angle (θ). This is precisely the configuration previously illustrated in Figure 3 except we have replaced the diffracting aperture with a scattering surface, and the geometry of the measurements has been folded about the reflecting plane. Hence, it should be no surprise, after our previous discussion of diffraction phenomena, that surfaces with well-behaved statistics exhibit scattering behavior that is shift-invariant with respect to incident angle when properly formulated in direction cosine space. The scattered intensity distribution illustrated on the observation hemisphere in Figure 12 thus becomes very skewed and asymmetrical as the angle of incidence is increased; however, when this data is divided by the cosine of the scattering angle and projected onto the plane of the scattering surface, the scattered radiance distribution does not change shape with incident angle. It merely shifts in direction cosine space while maintaining the symmetrical shape indicated in the figure.

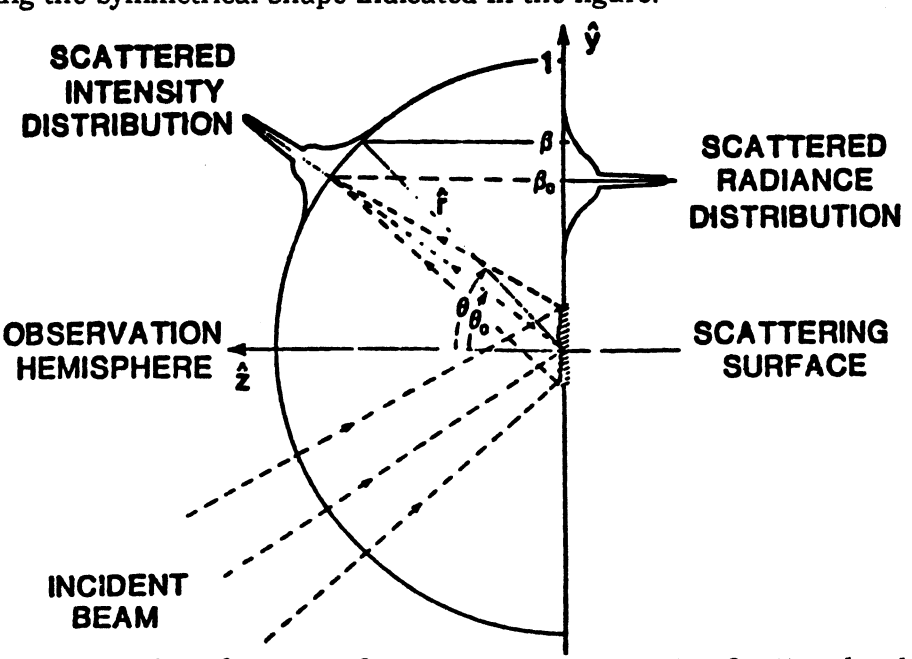

Figure 12. Geometrical configuration for scatter measurements. Scattered radiance is shift-invariant in direction cosine space for well-behaved surfaces.

Please note that β is the direction cosine of the position vector of the observation point and β_0 is the direction cosine of the position vector of the specularly-reflected beam. These direction cosines are obtained by merely projecting the respective points on the hemisphere back onto the plane of the sample and normalizing to a unit radius.

This shift-invariant behavior implies the existence of a "surface transfer function" which can be shown to relate the scattering properties to the surface characteristics. By describing surface scatter phenomena as a diffraction process in which the rough surface introduces random phase variations into the effective pupil function of the system, an analytical expression can be obtained for the transfer function of the scattering surface. Harvey has shown that if we assume a stationary process (i.e., a random, homogeneous, isotropic mirror surface), and a gaussian surface height distribution function, this transfer function is described by the following expression

$$H(x, y) = \exp\{ - (4\pi\sigma)^2 [1 - C(x/\ell, y/\ell)/\sigma^2]\} \qquad (14)$$

where σ^2 is the variance of the surface height distribution and $C(x/\ell, y/\ell)$ is the two-dimensional autocovariance function of the surface.[23] These parameters are illustrated schematically in Figure 13.

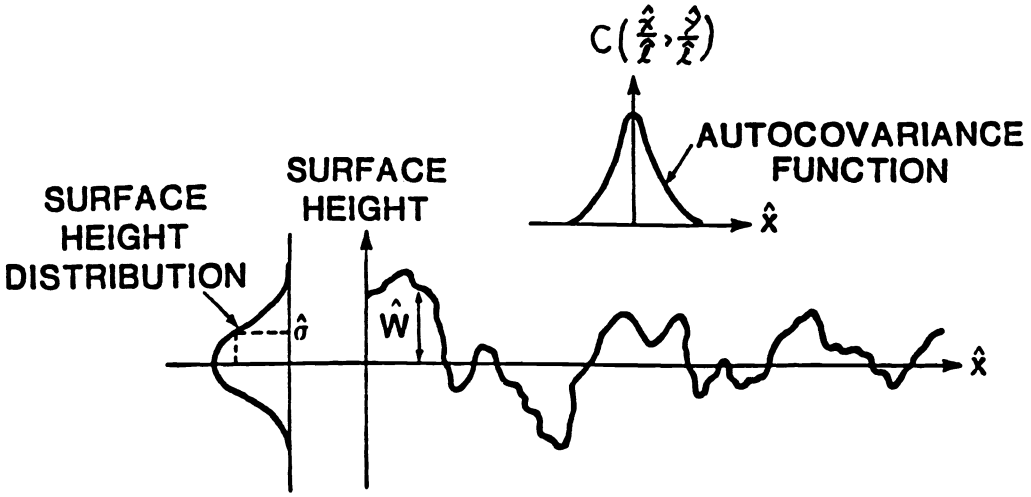

Figure 13. A surface profile and the relevant statistical parameters.

Considerable insight into the scattering process can now be obtained by considering the nature of this transfer function. The autocovariance function approaches the value σ^2 as the displacement approaches zero. The equivalent transfer function thus approaches unity as expected. As the displacement approaches infinity, the autocovariance function approaches zero and the equivalent transfer function approaches a plateau of height $\exp[- (4\pi\sigma)^2]$. The equivalent transfer function of the scattering surface can thus be regarded as the sum of a constant component and a bell-shaped component as shown in Figure 14a. Equation (14) can therefore be rewritten as

$$H(x, y) = A + B\, Q(x, y) \qquad (15)$$

where

$$A = \exp[- (4\pi\sigma)^2] \qquad (16)$$

$$B = 1 - \exp[- (4\pi\sigma)^2] \qquad (17)$$

and

$$Q(x, y) = \{\exp[(4\pi)^2\ C(x/\ell, y/\ell)] - 1\}/[\exp (4\pi\sigma)^2 - 1] \qquad (18)$$

The significance of this interpretation of the equivalent transfer function of the scattering surface is shown by the inferred properties of the corresponding "angle spread function". Since the transfer function is the sum of two separate components, the angle spread function of the scattering surface is the sum of the Fourier transforms of the two component functions

$$\mathcal{S}(\alpha, \beta; \hat{r}) = \mathcal{F}\{H(\hat{x}, \hat{y})\} = A\,\delta(\alpha, \beta; \hat{r}) + S(\alpha, \beta; \hat{r}) \qquad (19)$$

where the scattering function

$$S(\alpha, \beta; \hat{r}) = B\,\mathcal{F}\{Q(\hat{x}, \hat{y})\} \qquad (20)$$

The constant component of the transfer function transforms into a delta function, and the bell-shaped component transforms into a bell-shaped scattering function as illustrated in Figure 14. Hence the scattering surface reflects an incident beam of light as a specularly reflected beam of diminished intensity surrounded by a halo of scattered light. Furthermore , from the central ordinate theorem of Fourier transform theory, the relative power distribution between the specular component and the scattered component of the angle spread function are given by the quantities A and B respectively.

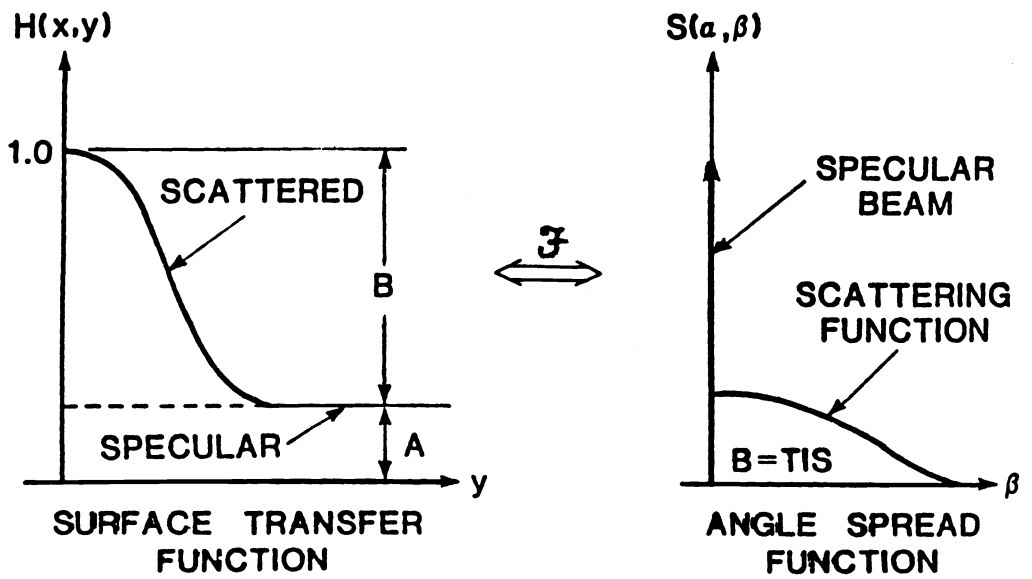

Figure 14. The surface transfer function and the associated angle spread function.

This transfer function characterization of scattering surfaces offers a simple means of determining the wavelength dependence of the scattered light distribution. Once the surface characteristics are known (whether from direct measurement or calculated from scattered light data), this theoretical model provides a simple method of predicting the scattering function at any desired wavelength. If we scale the wavelength by the factor **a**, the wavelength scaling law for smooth surfaces ($\sigma << \lambda$), is given by[23]

$$S(\alpha, \beta; a\lambda) = (1/a)^4\, S(\alpha/a, \beta/a; \lambda) \qquad (21)$$

Note that in addition to the $(1/a)^4$ change in magnitude, the width of the scattering function in direction cosine space is scaled by a factor **a**. This predicted behavior is experimentally verified in Figure 15 where the vertical and horizontal dashed lines correspond to the change in magnitude and the change in angular width of the scattering function.

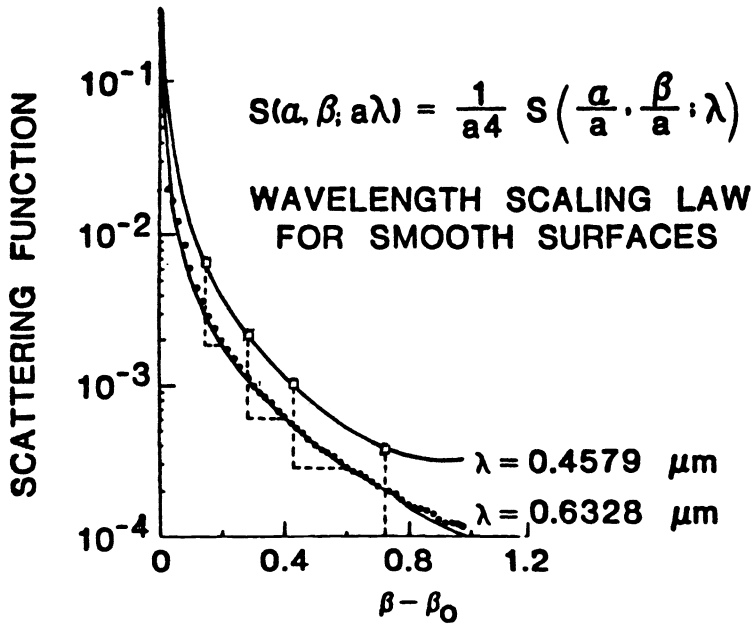

Figure 15. Wavelength dependence of the scattered light distribution.

It should be emphasized that both scattering measurements and surface topography measurements are band-limited (i.e., yield information about the surface irregularities over a finite band of spatial frequencies) and hence care must be taken when attempting to predict scattering behavior at one wavelength from scattering measurements at a different wavelength.[24] The angle of incidence can be varied to assure that the appropriate range of spatial frequencies are being sampled for predicting scattering characteristics of a given wavelength over a specific angular range (i.e., smaller angles than physically measurable due to mechanical and optical constraints) from measurements at a convenient wavelength and angular range.[25]

6. SUMMARY AND CONCLUSIONS

A review of linear systems theory and its highly successful application to the analysis of image forming systems including those with field dependent aberrations and image motion was first presented. A tutorial discussion then showed near-field scalar diffraction theory to be shift-invariant with respect to incident angle only when formulated in direction cosine space. Although it does not change the physics, there is tremendous benefit in convenience and insight by performing all wide-angle diffraction calculations in terms of the direction cosines of the propagation vectors.

Experimental surface scatter data from an optically polished and aluminized fused quartz sample was then shown to exhibit shift-invariant behavior in direction cosine space when scattered radiance (the BRDF is defined as reflected radiance divided by incident irradiance) rather than scattered intensity was plotted. This suggested that the application of linear systems theory and modern Fourier techniques might result in a theoretical model of scattering from optical surfaces that closely parallels the highly successful theory of isoplanatic imaging systems.

By describing surface scatter phenomena as diffraction from a random phase grating, an analytical expression for a surface transfer function which completely characterizes the scattering properties of well-behaved (random, homogeneous, isotropic, and a gaussian surface height distribution function) optical surfaces was presented. This transfer function was expressed only in terms of the rms roughness and the surface autocovariance function and therefore provides a simple solution to the inverse scattering problem of determining surface characteristics from scattered light measurements.

These Fourier techniques also provide the basis for deriving a wavelength scaling law for scattering behavior from smooth surfaces. This wavelength scaling law was presented and experimentally verified. Additional references were cited which also present experimental evidence that carefully applied wavelength scaling can be performed with confidence to predict scattering behavior at angles smaller than physically measurable.

General scattering surfaces which do not exhibit shift-invariance with respect to incident angle were also discussed. It was argued that the linear systems approach of modeling of surface scatter phenomena should not be abandoned because some samples of interest do not obey this simple model. Instead, a more regorous theoretical treatment should be used to determine the departure of the actual performance from the idealized behavior described by the model. This is precisely what has been done in modern image formation theory and has proven to be immensely useful, with the additional information provided by aberration theory to describe the departure of the actual behavior from the ideal behavior predicted by the system transfer function.

7. REFERENCES

1. Gary H. Hunt, Ed., *Radiation Scattering in Optical Systems*, Proc. SPIE 257 (1980).
2. S. Musikant, Ed., *Scattering in Optical Materials*, Proc. SPIE 362 (1982).
3. John C. Stover, Ed., *Scatter from Optical Components*, Proc. SPIE 1165 (1989).
4. J. D. Lytle and H. Morrow Eds., *Stray Light Problems in Optical Systems*, Proc. SPIE 107 (1977).
5. Robert P. Breault, Ed., *Generation, Measurement and Control of Stray Radiation III*, Proc. SPIE 384 (1983).
6. Robert P. Breault, Ed., *Stray Radiation IV*, Proc. SPIE 511 (1984).
7. Robert P. Breault, Ed., *Stray Radiation V*, Proc. SPIE 675 (1986).
8. Robert P. Breault, Ed., *Stray Light and Contamination in Optical Systems*, Proc. SPIE 967 (1988).
9. F. E. Nicodemus, "Reflectance Nomenclature and Directional Reflectance and Emissivity", Appl. Opt. **9**, 1474-5 (1970).
10. W. L. Wolfe, "Incident Angle Invariance in Surface Scatter", Proc. SPIE 1165 (1989).
11. J. M. Elson and J. M. Bennett, "Vector Scattering Theory", Opt. Eng. **18**, 116-124 (1979).
12. E. L. Church, H. A. Jenkinson, and J. M. Zavada, "Relationship between Surface Scattering and Microtopographic Features", Opt. Eng. **18**, 125-136 (1979).
13. Y. Wang and W. L. Wolfe, "Scattering from Microrough surfaces: Comparison of theory and Experiment", J. Opt. Soc. Am. 73, 1596-1602 (1983).
14. J. D. Gaskill, *Linear Systems, Fourier Transforms, and Optics*, Wiley, New York (1978).
15. R. V. Shack, "Outline of Practical Characteristics of an Image Forming System," J. Opt. Soc. Am. 46, 755 (1956).
16. E. Ingelstam, "Nomenclature for Fourier Transforms of Spread Functions," J. Opt. Soc. Am. 51, 1441 (1961).
17. F. D. Smith, "Optical Image Evaluation and the Transfer Function," Appl. Opt. 2, 335 (1963).
18. J. W. Goodman, Introduction to Fourier Optics, McGraw-Hill, New York (1968).
19. M. D. Rosenau, Jr., "Image-Motion Modulation Transfer Functions," Symposium on the Practical Application of Modulation Transfer Functions, SPIE, Inc. (1965).
20. W. Swindell, "A Noncoherent Optical Analog Image Processor," Appl. Opt. 9, 2459 (1970).
21. J. E. Harvey, "Fourier Treatment of Near-field Scalar Diffraction Theory", Am. J. Phys. **47**, 974 (1979).
22. R. N. Bracewell, *The Fourier Transform and its Applications*, McGraw-Hill, New York (1965).
23. J. E. Harvey, "Light-Scattering Characteristics of Optical Surfaces," Ph.D Dissertation, U. Arizona (1976).
24. J. C. Stover, J. Rifkin, D. R. Cheever, K. H. Kirchner and T. F. Schiff, "Comparison of Wavelength Scaling Data to Experiment", Proc. SPIE 967, 44-49 (1988).
25. C. L. Vernold, "Application and Verification of Wavelength Scaling for Near Specular Scatter Predictions", Proc. SPIE 1165 (1989).